CHEMICAL ENGINEERING TRANSACTIONS
VOL. 94, 22
A publication of AIDIC
The Italian Association of Chemical Engineering
Online at www.cetjournal.it
Guest Editors: Petar S. Varbanov, Yee Van Fan, Jiří J. Klemeš, Sandro Nižetić

ISBN 978-88-95608-93-8; **ISSN** 2283-9216
DOI: 10.3303/CET2294205

Numerical Analysis of an Air Humidification System Using Computational Fluid Dynamics

Mohammadreza Zarrabi[a], Mohammad Pourhoseinian[a], Seyedmehdi Sharifian[a], Neda Asasian-Kolur[a,b], Bahram Haddadi[b], Christian Jordan[b], Michael Harasek[b]

[a]Fouman Faculty of Engineering, College of Engineering, University of Tehran, P. O. Box 43515-1155, Fouman 43516-66456, Iran.
[b]Technische Universität Wien, Institute of Chemical, Environmental and Bioscience Engineering, Getreidemarkt 9/166, A-1060 Vienna, Austria.
bahram.haddadi.sisakht@tuwien.ac.at

Air humidification systems are in demand in many industrial and municipal sectors. Bubble columns are one of the most common forms of laboratory-scale humidifiers. Many operating parameters affect the performance of these systems, such as bubbler geometry, gas flow rate, temperature, the water level in the bubbler, and nozzle type. Since considering all these factors in an experimental system is costly, predicting performance by a computational fluid dynamics model is essential. In the present study, a laboratory-scale bubble column was simulated, and the effect of operating parameters was determined in terms of relative humidity at the outlet. In addition, the hydrodynamic fluid transfer from the nozzle to the outlet was thoroughly evaluated. An acceptable agreement was obtained between the experimental and model data, allowing further investigation on other important variables. Among the geometrical parameters, the ratio of water height to column diameter and nozzle type affected system performance by about 4 % and 20 %. Changing the flow rate and water temperature also affected the humidification process by 15 % and 16 %. The model scheme can be useful in developing and performing humidification systems before practical application.

1. Introduction

Adding moisture or water vapor to the air stream without changing the dry bulb temperature is called the humidification process. One of the most popular applications of the process of cooling and humidification is air conditioning/cooling. In this process, moisture is transferred to the air by passing a stream of water at a temperature lower than the air's dry-bulb temperature (Cao et al., 2020). Water evaporates by releasing heat into the stream during this process. As the air stream absorbs the evaporated water, its moisture content and humidity increase. Since the temperature of the absorbed moisture is lower than the air dry-bulb temperature, the overall temperature of the air decreases at the same time (Davis et al., 1995).
There are many different types of humidifiers. The choice of a particular method depends on the size of the process, the availability of water, the budget, the degree of control required, and the methods used to treat and distribute the air (Cao et al., 2020). Since the 1960s, when the humidification process in a non-adiabatic system was studied experimentally (Stewart and Bruley, 1967), this topic has received considerable attention until today. El-Agouz and Abugderah studied the humidification process by air flowing through seawater (El-Agouz and Abugderah, 2008). They determined the behaviour of humid air through single-stage heating and humidification processes. For this purpose, they studied the effects of operating conditions such as water temperature, pressure difference, air velocity, and supply air temperature on vapour fraction difference and humidification efficiency. In another study, the desiccant solution's humidification/dehumidification process by blowing air through a calcium chloride solution was studied under various operating conditions such as temperature, humidity, and solution levels (Kabeel, 2010). Feng et al. (2018) investigated the influences of the humidification process on the indoor environment in an isothermal chamber. The results showed that a portable ultrasonic humidifier increases humidity while decreasing temperature and when the relative humidity was increased from 34 % to 60 %, the air temperature was reduced by 1.5 °C. In addition, Zhang et al. (2020) studied

Paper Received: 13 April 2022; Revised: 03 June 2022; Accepted: 12 June 2022
Please cite this article as: Zarrabi M., Pourhoseinian M., Sharifian S., Asasian-Kolur N., Haddadi B., Jordan C., Harasek M., 2022, Numerical Analysis of an Air Humidification System Using Computational Fluid Dynamics, Chemical Engineering Transactions, 94, 1231-1236 DOI:10.3303/CET2294205

the process of air humidification for the humid air turbine cycle using a two-phase measurement system. This research thoroughly explored the effects of water/air ratio and water inlet temperature on the humidification process.

Computational Fluid Dynamics (CFD) is a technique that uses computer-based numerical analysis and algorithms to predict, analyse, and solve problems involving the flow behaviour of fluids and heat transfer systems. This technique can significantly reduce the cost of evaluation compared to empirical testing. Saeed et al. (2016) proposed a CFD model for a humidification/dehumidification distillation process (Saeed et al., 2016). This model was developed to predict the velocity, temperature, and moisture concentration distribution and calculate the water evaporation rate; it was based on the numerical solution of the conservation equations for mass, momentum, energy, and species considering the Boussinesq approximation. In addition, Al-Abbasi et al. (2019) investigated a mathematical model of a solar humidifier. It was found that in addition to the heat flux and airflow rate, the height of the humidification channel also affects the system performance. For the different heat fluxes, it was reported that the maximum evaporation rate is achieved at the smallest duct height and flow rate (Al-Abbasi et al., 2019). Pourhoseinian et al. (2021) investigated a CFD model for moisture transfer between two airflows through a membrane heat exchanger. To this end, sensible and latent effectiveness, water emission rate, energy recovery, and pressure drop were assumed as performance parameters, and operating conditions including the number of channels on each side of the module, airflow rate, and the effects of flow configuration changes on these parameters were studied (Pourhoseinian et al., 2021).

Humidification and dehumidification are two common processes used either in domestic applications such as HVAC (Asasian-Kolur et al., 2022) or in industrial applications such as fuel cells and methanation processes (Murathathunyaluk et al., 2019). The current study investigates the humidification process experimentally and numerically using a bubbler with a specific characterization. First, the effects of water temperature and flow rate were investigated by experimental tests. Subsequently, to determine the effect of other costly parameters, further studies were conducted through CFD modelling to estimate the effects of the nozzle type's influence and the bubbler's geometry under adiabatic conditions.

2. Material and methods

2.1 Experimental set-up

Figure 1 shows that the humidifier consists of a compressor, a cylinder bubbler, a valve, a thermocouple, a thermometer, a barometer, a humidity meter, and a flow meter. The air is supplied by a compressor (Active AC1350S, 50 L), and its flow is adjusted by a flow meter (LZB-DK, 0.5-5 L/min). Then the humidity and temperature of the stream are measured by a temperature-humidity meter (ENDA EHTC7425A), and pressure is shown by a pressure gauge (Wika, EN 837-1, 0-4 bar). The airflow is then introduced into the bubbler (SS 304, thickness: 4 mm, volume: 2 L) through a pipe (stainless steel, ¼ inch) and then directed through a dense nozzle (Swagelok® SC -11 gas filter) from the bottom the cylinder into the water medium. The humid air is then passed through the outlet, and its properties are measured again. In order to change the water temperature in the bubbler, a thermocouple (YOURGRILL®) is used. In the experimental study, the airflow and water temperature levels were chosen in the range of 0.5-1 L/min and 20-80 °C to investigate their effects on humidification performance.

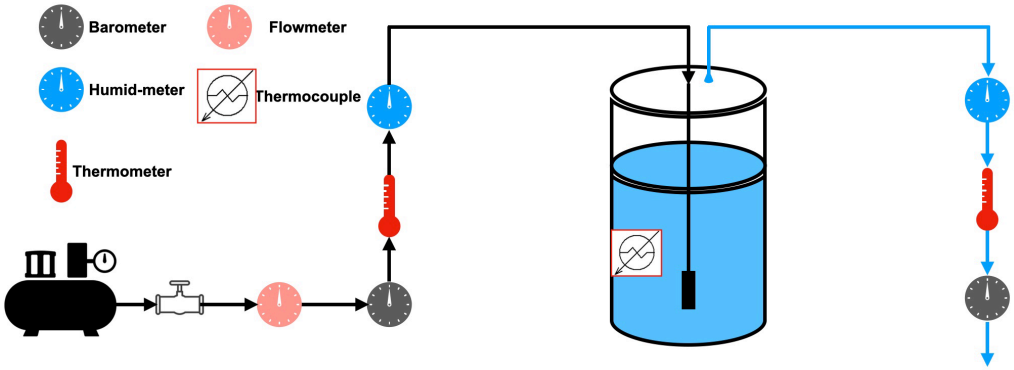

Figure 1: A schematic representation of the air humidification process

2.2 Numerical method

The advent of powerful computers with high memory and processing capacity has provided the basis for computational fluid dynamics to predict flow patterns and velocity profiles under various designs and operating

conditions. Figure 2a shows the cylinder bubbler's geometry and the selected domain's key specifications for 2-D computational analysis. As can be seen, the height and diameter of the bubbler are 26 and 9 cm. The computational grid was created using the MESH tool in ANSYS @ FLUENT 2021R2. Figure 2c and 2b show the grids generated throughout the domain and near the nozzle area. It can be seen that the map elements were implemented not the paving elements. The generation of quadrangular patches instead of triangular elements decreases the computational cost and increases the accuracy of the numerical solution. The grid density is relatively high near the centre to account for the relatively high air flows and pressure gradients in the centre line.

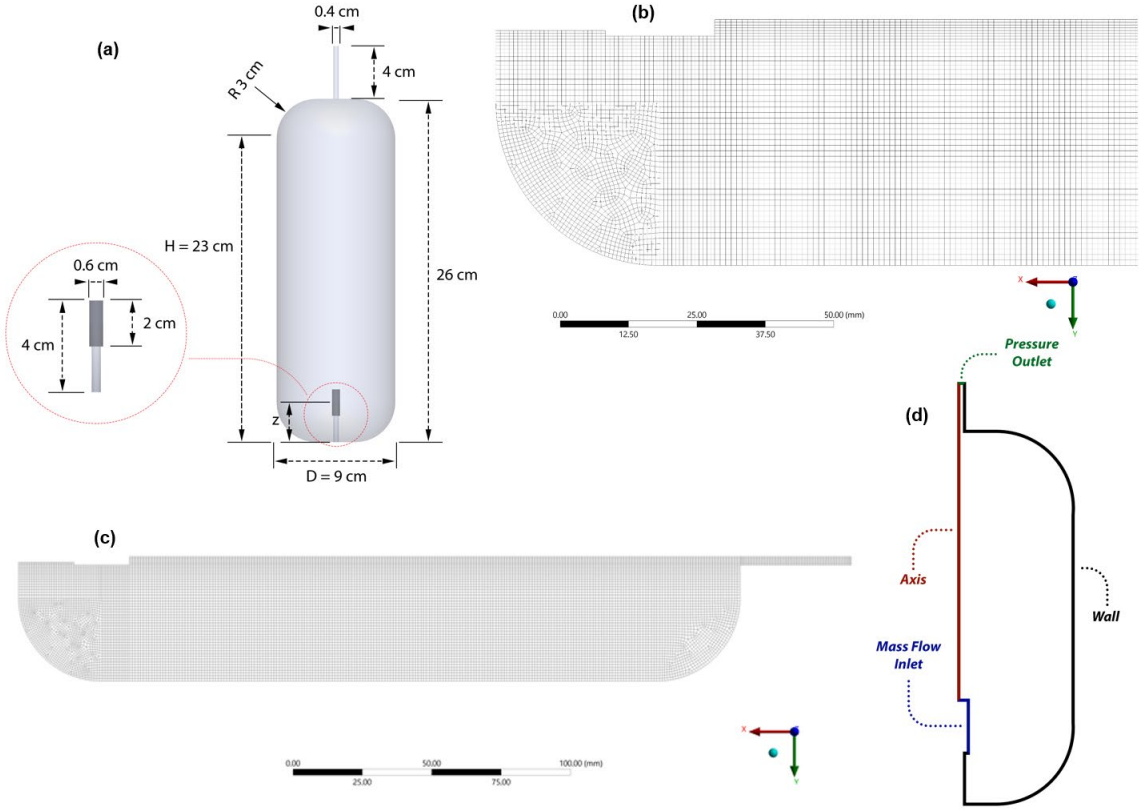

Figure 2: (a) Schematic representation of a cylindrical bubble column, (b) grid near the nozzle, (c) grid and elements of the entire computational domain, (d) schematic representation of the boundary conditions for the system

An adiabatic condition was considered in the CFD model via ANSYS FLUENT. In addition to the multiphase model, the Navier-Stokes equation was also computed numerically. The Eulerian model was chosen as one of the most commonly used models for bubble columns (Sokolichin et al., 2004), which have a high number of bubbles despite a low gas content. The solution method was based on a single pressure for both phases, solving the continuity and momentum equations for each phase. The Symmetric model was used among the interphase-drag coefficient functions that can be applied to multiphase regimes in the Eulerian model. In general, drag coefficient models described in terms of local Reynolds numbers are used to determine phase coupling through the interphase exchange terms. The Reynolds number was in the laminar flow range (in the range of 200-300). Raoult's law was also applied stating that the vapor pressure of a solvent over a solution is equal to the vapor pressure of the pure solvent at the same temperature, scaled by the mole fraction of the solvent. The selected solution methods and schemes are listed in Table 1. Schematic representation of the boundary conditions for the system is also shown in Figure 2d.

Table 1: Numerical methods

Pressure-Velocity Coupling Scheme	Phase Coupled SIMPLE
Discretization Methods	
Gradient	Least Squares Cell Based

Pressure	PRESTO!
Momentum	First Order Upwind
Volume Fraction	Compressive
Species	Second Order Upwind
Transient Formulation	Second Order Implicit
Multiphase Model	Eulerian
Number of Eulerian Phases	2
Drag Coefficient	Symmetric
Surface Tension Coefficient	0.072 N/m
Mass Transfer Mechanism	Species Mass Transfer
Species Mass Transfer Model	Raoult's Law
Interphase Mass Transfer Coefficient	Ranz-Marshall

3. Result and discussion

Figure 3 shows the experimental results indicating the relative humidity of the outlet stream as the bubbler water temperature changes from 10 to 70 °C. It can be seen that the relative humidity increases as the water temperature increases. The trends of relative humidity changes were studied with an airflow rate of 500 and 1,000 mL/min at the room air temperature of 17 °C and pressure of 1 atm. It can be seen that the relative humidity follows the same pattern at both volume flow rates and that increasing the water temperature has a positive effect on the humidity obtained. It can also be seen that a higher flow rate results in higher humidity in all temperature ranges.

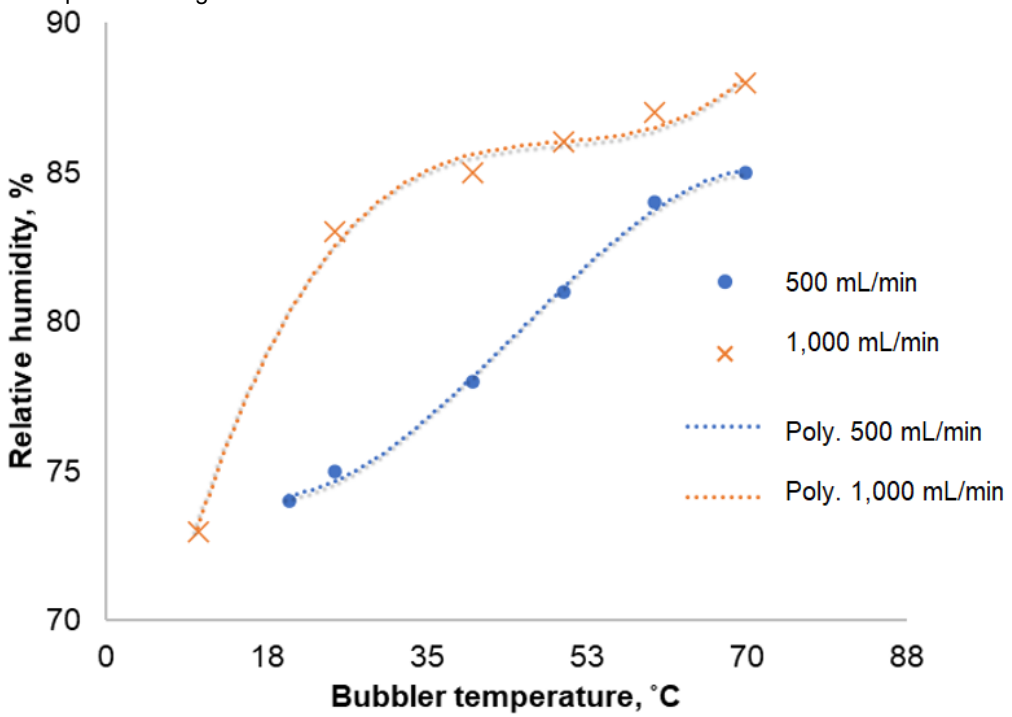

Figure 3: Experimental results showing the changes in relative humidity versus water temperature at 500 and 1,000 mL/min air volume flow rates

In order to obtain accurate and precise results with less computational time, it seems very important to find the optimal element regions. A grid independence test was performed with different numbers of elements to determine the minimum number of elements required to obtain sufficiently accurate results. Figure 4 shows the differences between the accuracy of the simulation results at different element numbers used in the grid independence study. It can be seen that the vapour mass fraction in the outlet stream reaches a constant value when the element number is increased from 14,038 to 17,572 when the airflow rate is 500 mL/min. Therefore, 14,038 was the optimum element number for further numerical investigations.

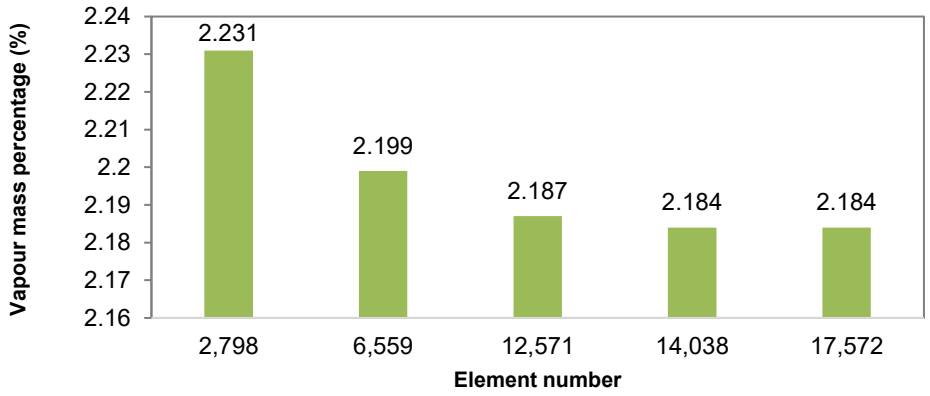

Figure 4: Grid independence results

Verification and validation are the primary means of evaluating the accuracy and reliability of computational results. Validation evaluation is concerned with determining whether computational results are consistent with physical reality. It can be performed by comparing experimental results with calculated data. Table 2 compares calculated results with experimental values when the flow rate varies from 500 to 1,000 mL/min. It can be clearly seen that the maximum relative error is 11.5 %. The simulation results show good agreement with the empirical data. This discrepancy between the computational results and the experiments may be due to some non-ideal conditions in the experimental operation and the assumptions considered in the CFD analysis. One of the problems related to the experimental analysis is that the humidity/temperature gauge is not accurately placed exactly at the cylinder outlet, and this distance (even a few centimetres) can change the results. In addition, the adiabatic assumption considered in the CFD analysis is an ideal condition that cannot be achieved in practice.

Table 2: Validation of CFD results and experimental data

Flow rate, mL/min	RH, % (calculated)	RH, % (measured)	Relative Error, %
500	88.14	78	11.5
1,000	75.67	83	9.7

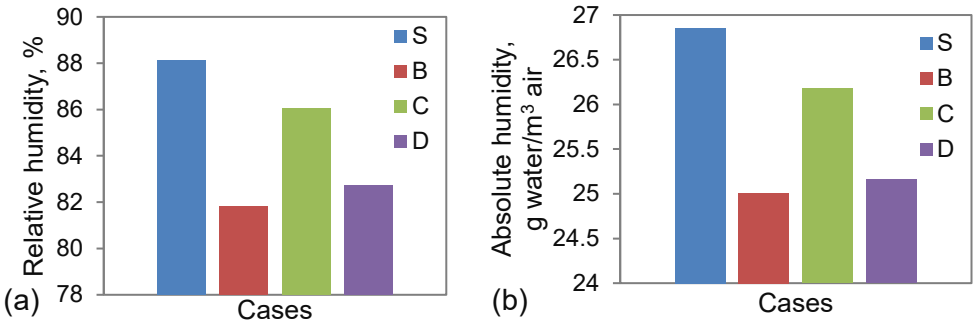

Figure 5: CFD results for different cases: S: standard conditions (based on Figure 2a); B: effects of changing nozzle position; C: effects of changing bubble size; D: effects of changing water level on humidifier performance of (a) relative humidity and (b) absolute humidity

In order to investigate design parameters such as the nozzle type, the nozzle position in the bubbler, and the cylinder shape, a CFD analysis was performed. The results are presented (Figure 5) in terms of relative and absolute humidity in the bubbler outlet. The simulation cases were based on the standard type designated S (Z/H = 0.33, bubble size = 0.7 mm), B (Z/H = 1.66, bubble size = 0.7 mm), C, (Z/H = 0.33, bubble size = 1.4 mm), and D (Z/H = 0.33, bubble size = 0.7 mm, water level 1/2). Among all the design parameters, it can be observed that the change of nozzle position and the water level has a much greater influence on the humidifier performance in terms of absolute and relative humidity than the bubble size, which is completely dependent on the nozzle type in the adiabatic condition.

4. Conclusion

A cylinder bubbler humidifier was experimentally tested at specific dimensions, geometries, operating volume flow rates, and water temperatures. A mathematical model to evaluate the humidifier's performance was developed and validated against the experimental results. The results from CFD showed good agreement with the experimental data. Several design variables such as nozzle type, flow rate, nozzle position, and cylinder size that affect the performance of the humidification process were investigated. The airflow rate was found to have the most significant effect on the humidity of the outlet air produced. In addition, among the design parameters, nozzle position, water level, and bubble diameter affected the system's performance. This work can be extended by introducing a non-adiabatic model under different operating conditions.

References

Al-Abbasi O., SARAÇ B., Ayhan T., 2019. Experimental investigation and CFD modeling to assess the performance of solar air humidifier. International Journal of Heat and Technology, 37, 357–364.

Asasian-Kolur N., Sharifian S., Haddadi B., Pourhoseinian M., Mousazadeh Shekarbaghani Z., Harasek M., 2022. Membrane-based enthalpy exchangers for coincident sensible and latent heat recovery. Energy Conversion and Management, 253, 115144–115169.

Cao G., Railio J., Curd E.F., Hyttinen M., Liu P., Mathisen H.M., Belkowska-Woloczko D., Justo-Alonso M., White P., Coxon C., Wenaas T.A., 2020. Air-handling processes, Chapter In: H D Goodfellow, R Kosonen (Eds.), Industrial Ventilation Design Guidebook, Vol 1. Academic Press, London, UK, ISBN: 978-0-12-816780-9, 417–496.

Davis P.D., Parbrook G.D., Kenny G., 1995. CHAPTER 12 – Humidification, Chapter In: P D Davis, G D Parbrook, G N C Kenny (Eds.), Basic Physics and Measurement in Anaesthesia. Vol 1, Butterworth-Heinemann, Oxford, UK, ISBN: 0-7506-1713-6, 146–157.

El-Agouz S.A., Abugderah M., 2008. Experimental analysis of humidification process by air passing through seawater. Energy Conversion and Management, 49, 3698–3703.

Feng Z., Zhou X., Xu S., Ding J., Cao S.-J., 2018. Impacts of humidification process on indoor thermal comfort and air quality using portable ultrasonic humidifier. Building and Environment, 133, 62–72.

Kabeel A.E., 2010. Dehumidification and humidification process of desiccant solution by air injection. Energy, 35, 5192–5201.

Murathathunyaluk S., Junjiewchai J., Kitchaiya P., 2019. Effect of regeneration conditions on dehumidification desiccant packed bed. Chemical Engineering Transactions, 76, 715–720.

Pourhoseinian M., Asasian-Kolur N., Sharifian S., 2021. CFD investigation of heat and moisture recovery from air with membrane heat exchanger. Applied Thermal Engineering, 191, 116911–116924.

Saeed A., Antar M.A., Sharqawy M.H., Badr H.M., 2016. CFD modeling of humidification dehumidification distillation process. Desalination, 395, 46–56.

Sokolichin A., Eigenberger G., Lapin A., 2004. Simulation of buoyancy driven bubbly flow: Established simplifications and open questions. AIChE Journal, 50, 24–45.

Stewart R.R., Bruley D.F., 1967. Thermal dynamics of a distributed parameter nonadiabatic humidification process, AIChE Journal, 13, 793–796.

Zhang Q., He M., Wang Y., Weng S., 2020. Experimental analysis of the air humidification process for humid air turbine cycle using a two-phase measurement system. Applied Energy, 279, 115892–115904.